

Origin of the Formation of Nanoislands on Cobalt Catalysts during Fischer–Tropsch Synthesis

Arghya Banerjee,[†] Alexander P. van Bavel,[§] Herman P.C.E. Kuipers,[§] and Mark Saeys^{*,‡}

[†]Department of Chemical and Biomolecular Engineering, National University of Singapore, Singapore 117576

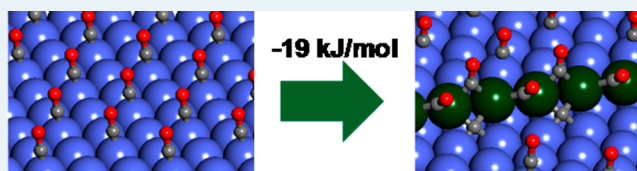
[§]Shell Technology Centre Amsterdam, P.O. Box 38000, 1030 BN Amsterdam, Netherlands

[‡]Laboratory for Chemical Technology, Ghent University, Technologiepark 914, 9052 Gent, Belgium

ABSTRACT: Cobalt catalysts undergo a massive reconstruction under Fischer–Tropsch conditions, resulting in the formation of uniform nanoislands. It is unclear what drives the formation of these islands, since it is highly unfavorable for clean surfaces. Using density functional theory, we show that the formation of islands and steps is driven by the embedding of carbon in an unusual square-planar form at the B5 step sites.

Though carbon is not a typical oxidant for metals, it oxidizes cobalt at those sites. This strengthens CO adsorption, which further favors the formation of islands and steps. The oxidation of cobalt by carbon is predicted to be experimentally detectable as a 2 eV shift in the Co 2p binding energy.

KEYWORDS: catalysis, cobalt, Fischer–Tropsch synthesis, square planar carbon, nanoislands



INTRODUCTION

The structure of heterogeneous catalysts under reaction conditions often differs dramatically from their ideal clean structure,^{1–6} challenging the validity of model studies that assume ideal catalyst structures. A striking example is the formation of quasi-uniform nanoislands with a height of one atomic layer and containing less than 50 Co atoms when a Co(0001) single crystal is exposed to CO and H₂ under Fischer–Tropsch reaction conditions of 4 bar and 523 K.¹ The formation of nanoislands greatly increases the number of surface “defect” sites, which have been proposed as the catalytically active sites for Fischer–Tropsch synthesis.^{7,8} Insight into the formation, the structure, and the coverage of these nanoislands would therefore be an important step toward controlling the activity and selectivity of Fischer–Tropsch synthesis, a major industrial process for the production of clean fuels. This massive reconstruction of the cobalt catalyst under reaction conditions is however puzzling because island formation is highly unfavorable on clean cobalt surfaces. Moreover, the nanoislands only form under reaction conditions and were not observed by *in situ* STM at 10 mbar and for a high H₂/CO ratio of 40.⁹

The driving force and conditions required for the formation of the nanoislands remain controversial. Wilson and De Groot first observed the formation of nanoislands and speculated that strong adsorption of dicarbonyl species at the “defect” sites drives their formation.¹ Recently, surface carbidic species have been suggested as the restructuring agents¹⁰ because calculations have shown that carbon binds strongly at step sites.^{11–14} A number of theoretical studies using *ab initio*^{15,16} and molecular dynamics methods¹⁷ have found that high carbon coverages can reconstruct Co terraces to form a surface carbide, but not nanoislands. For example, Zhang et al.¹⁷ proposed that

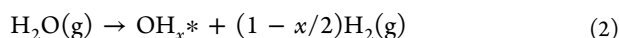
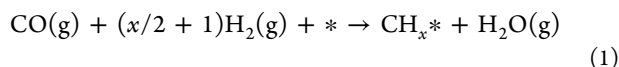
strong C adsorption increases Co–Co distances, resulting in surface stress, in agreement with the results of Tan et al.¹¹ This surface stress can then be reduced by the formation of step sites and islands, linking the formation of a surface carbide to the formation of steps and islands. Valero et al.¹⁶ also attributed the formation of a surface carbide to the strong C binding energy in the carbide and at subsurface sites. In a combined experimental and theoretical study, Tan et al.¹¹ found that both a graphene overlayer and a p4g surface carbide are thermodynamically stable under Fischer–Tropsch conditions and can grow from step edges on Co(111) terraces. Dosing and decomposing 0.5 ML ethylene at 630 K indeed reconstructs the Co(0001) surface forming a surface carbide,¹⁸ in agreement with theoretical predictions,^{11,15,16} but it does not lead to the formation of nanoislands. The specific conditions that lead to the formation of the catalytic nanoislands therefore remain unclear. Also, a high CO coverage of around 50% is measured under Fischer–Tropsch conditions.^{19,20} However, the effect of strongly adsorbed CO on the catalyst structure was not considered in these earlier studies. Here we present a computational study to address the thermodynamic origin and conditions for the experimentally observed formation of nanoislands under Fischer–Tropsch conditions. The effect of the high CO surface coverage on the stability of Co terraces and the combined synergistic effect of C and CO adsorption on the formation of nanoislands are addressed for the first time. We show what species can and should bind to Co under reaction conditions to facilitate the formation of steps and islands.

Received: December 30, 2014

Published: July 2, 2015

■ COMPUTATIONAL METHODS

Periodic spin-polarized density functional theory calculations were performed using the revised Perdew–Burke–Ernzerhof (revPBE) functional²¹ including nonlocal vdW-DF correlation,^{22,23} a plane-wave basis set with a cutoff kinetic energy of 450 eV, and the projector-augmented wave method,²⁴ as implemented in the Vienna Ab-initio Simulation Package (VASP).^{25,26} The thermodynamic stability of CO, CH_x, and OH_x adsorbates relative to a CO, H₂, and H₂O gas phase reservoir was evaluated from the reaction Gibbs free energy for eqs 1 and 2 under Fischer–Tropsch conditions (500 K, 20 bar, 60% conversion), and includes the effects of pressure, composition, and temperature²⁷ (eqs 3 and 4).



$$\Delta G_{\text{CH}_x}(T, p) = \Delta G^0(500 \text{ K}) + RT \ln(p_{\text{H}_2\text{O}}/p_{\text{CO}}p_{\text{H}_2}^{x/2+1}) \quad (3)$$

$$\Delta G_{\text{OH}_x}(T, p) = \Delta G^0(500 \text{ K}) + RT \ln(p_{\text{H}_2}^{1-x/2}/p_{\text{H}_2\text{O}}) \quad (4)$$

The Gibbs free energy for gas phase and adsorbed species was calculated by combining electronic and zero-point DFT energies with enthalpy corrections and entropies from frequency calculations for the full structures. Co terraces were modeled as a three-layer $p(3 \times 3)$ slab with an optimized lattice constant of 3.56 Å and an interslab spacing of 10 Å. Step sites were modeled using a three-layer $p(2 \times 8)$ slab where four rows of Co atoms were removed from the top layer. The Brillouin zone was sampled with a $(3 \times 3 \times 1)$ Monkhorst–Pack grid. IR intensities were calculated using density functional perturbation theory,²⁸ whereas C 1s and Co 2p binding energies were computed using the final state approximation.^{29,30}

■ RESULTS AND DISCUSSION

Step creation and island formation are highly unfavorable for the clean Co(111) surface. Creating a pair of B5 and F4 step sites by breaking a large (111) terrace into two smaller terraces costs 85 kJ/mol (Figure 1). Note that the symmetry of the fcc

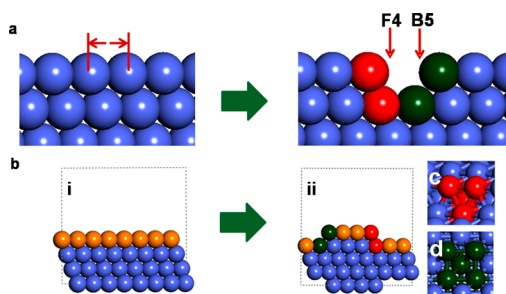


Figure 1. (a) Creation of a pair of F4 and B5 sites on Co(111) terraces. (b) Procedure to calculate the step creation energy. In a $p(2 \times 8)$ Co(111) unit cell, 4 rows are moved from the top layer (i) to the bottom layer (ii), creating 4 F4 step sites (red, c) and 4 B5 step sites (green, d) per unit cell. Note that 8 rows of terrace sites (i) form 5 rows of terrace sites in (ii) (indicated in orange), 1 row of B5 sites and 1 row of F4 sites. The energy difference between (i) and (ii) per unit cell, 340 kJ/mol, leads to a step creation energy of 85 kJ/mol per pair of step sites.

lattice leads to pairs of B5 and F4 sites in this procedure. Creating a step formally corresponds to breaking two Co–Co bonds, and the calculated step creation energy of 85 kJ/mol leads to a Co–Co bond energy of 43 kJ/mol. This value corresponds to a bulk cohesive energy of 510 kJ/mol, in reasonable agreement with the calculated bulk cohesive energy of 445 kJ/mol (experimentally 424 kJ/mol³¹). In this process, the number of adsorption sites decreases: three rows of terrace sites are converted to one row of B5 sites and one row of F4 sites. Since various carbon-containing species adsorb strongly on Co,^{11–17} it is natural to ask whether strong adsorption and high coverage at the new step sites could overcome the large energy penalty to create steps. To evaluate the effect of adsorbates, the stability of C, CH, and CH₂ at the steps (Figure 2), as well as the adsorption of CO on terraces and steps

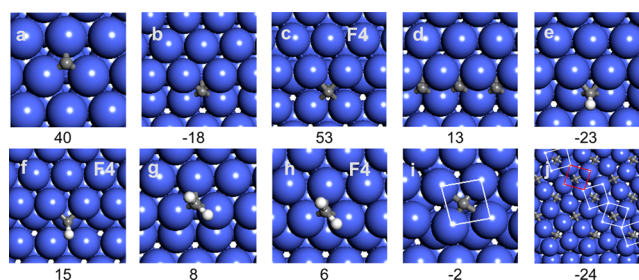


Figure 2. Thermodynamic stability (kJ/mol) of CH_x species on terrace and stepped Co surfaces relative to a syngas reservoir at 500 K, 20 bar, 60% conversion. (a) hcp hollow terrace site; (b) B5 site, 50% step coverage; (c) F4 site, 50% step coverage. Note that the edge atoms of the upper terrace shift to convert the 3-fold F4 site (Figure 1c) to a 4-fold site due to the stability of square-planar carbon; (d) B5 site, 100% step coverage. Addition of a second carbon is highly unfavorable; (e) CH at B5 step site, 50% coverage; (f) CH at F4 step site, 50% coverage; (g) CH₂ at B5 step edge, 50% coverage; (h) CH₂ at F4 step edge, 50% coverage; (i) p4g clock carbide at the step edge; (j) extended p4g clock carbide. Though the stability of the carbide depends on the width of the terrace,¹¹ the stability per carbon rapidly converges to a value of –24 kJ/mol (value for fourth carbon atom, indicated by red square). Co atoms are blue, C gray, and H white.

(Figure 3) was computed to find a combination that could overcome the step creation penalty. The calculations show that C and CH bind strongly at the 4-fold B5 step sites with stabilities of –18 and –23 kJ/mol, respectively. Thermodynamic stabilities are defined as reaction Gibbs free energies relative to a synthesis gas reservoir under Fischer–Tropsch conditions and fully account for the effect of temperature, pressure, and composition eqs 1–4. In particular, C binds 58 kJ/mol stronger at the 4-fold B5 site than at a hollow site on Co terraces (Figure 2a) and 71 kJ/mol stronger than at the 3-fold F4 site (Figure 2c). Note that the unusual stability of carbon at 4-fold sites forces the upper atoms of the F4 step to move significantly to create 4-fold sites. Hydrogenation of C to CH is only marginally favorable at the B5 sites. On Co terraces, hydrogenation of C to CH is highly favorable by 53 kJ/mol, illustrating the unique stability of the naked carbon at the B5 sites. CH₂ adsorbs preferably at the edge site (Figure 2g,h) and is unstable relative to C and to CH at the B5 site. At the 4-fold B5 sites, carbon binds in an unusual square-planar geometry. The stability of square-planar carbon at the B5 sites was analyzed by Nandula et al.³² and attributed to the local aromaticity of the square-planar “Co₄C” motif. Chemical bonding in metal clusters containing square-planar carbon is

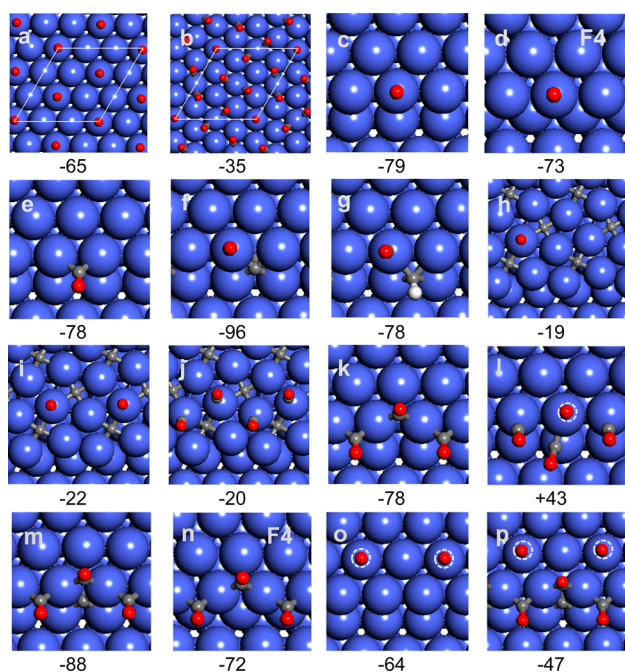


Figure 3. Adsorption Gibbs free energy of CO at terraces and step sites (500 K, 4.4 bar CO). The Gibbs free energies account for the adsorption entropy loss and are therefore about 60 kJ/mol lower than adsorption energies. (a) $\sqrt{3} \times \sqrt{3}$ -CO structure, the stable structure on Co terraces under Fischer–Tropsch conditions; (b) $(2\sqrt{3} \times 2\sqrt{3})$ -7CO structure, high coverage structure; (c) B5 step, 50% coverage; (d) F4 step, 50% coverage; (e) B5 step, 50% coverage, bridge sites; (f) B5 step with 50% carbon; (g) B5 step with 50% CH; (h) p4g carbide, low coverage; (i) p4g carbide, intermediate coverage; (j) p4g carbide, high coverage; (k) B5 edge, 100% CO coverage. Adsorption at top sites is not stable for this coverage; (l) B5 edge, 150% CO coverage. Adsorption free energy for the addition of CO molecules to structure 3k; (m) B5 step with 50% carbon, 100% CO coverage; (n) F4 step, 100% CO coverage; (o) next to a B5 step, 50% CO coverage for second row; (p) next to a C/CO-covered B5 step, 50% CO coverage for second row, adsorption free energy for the addition of CO molecules (circled) to structure 3m.

well-understood, and the hunt for clusters containing square-planar C, N, and Si is indeed very active.^{33–37} Here we demonstrate that the stability of this unusual square-planar carbon also plays a crucial role in the structure and activity of industrial catalysts.

Increasing the carbon step coverage to 100% by occupying neighboring B5 sites is unfavorable, with a differential Gibbs free energy of +44 kJ/mol for adsorbing a carbon atom between two occupied B5 sites (Figure 2d), leading to an average stability of +13 kJ/mol for a carbon coverage of 100%. Indeed, when carbon occupies neighboring B5 sites, aromaticity is destroyed.³² The saturation carbon coverage at B5 steps is hence only 50% under Fischer–Tropsch conditions, and B5 sites remain free and available for reaction. Another structure with square-planar carbon is the p4g-clock surface carbide. p4g surface carbides were first characterized on Ni(100),³⁸ and they have also been predicted on Co surfaces.^{11,15,16} The (111) surface carbide in Figure 2j grows from the step edge and slightly expands the (111) terrace, introducing strain. The reconstruction cost is largest for carbon next to the step (Figure 2i) and gradually decreases as the surface carbide grows. The stability eventually converges to about –24 kJ/mol for a width of five rows (Figure 2j).¹¹ Subsurface carbon was found to be at

least 60 kJ/mol less stable than the surface carbide under Fischer–Tropsch conditions.

The high CO pressure and relatively low temperature under Fischer–Tropsch conditions lead to a high CO coverage. Experimental and theoretical studies have reported CO coverages around 50% during Fischer–Tropsch synthesis.^{19,20} A thermodynamic analysis of the adsorbate-induced island and step formation should hence consider the CO coverage on the terraces before reconstruction, and adsorption at the step sites that are created by the reconstruction, as illustrated in Figure 4.

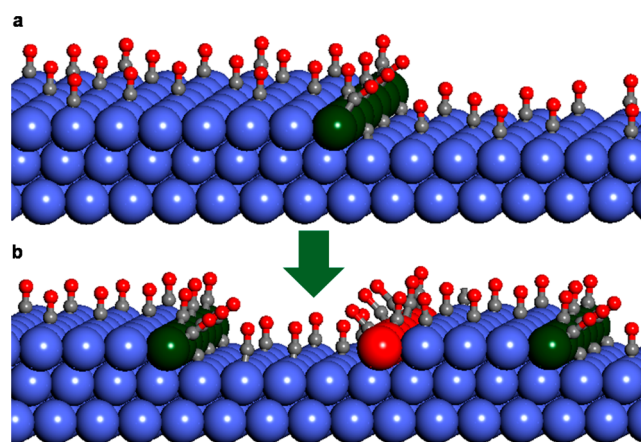


Figure 4. Formation of step sites under FT conditions. CO-covered Co terraces (a) break up, creating additional step sites (b). Although the creation of step sites (Figure 1) and the desorption of CO from the (terrace) sites costs energy, the adsorption of a high (100%) coverage of CO and square-planar carbon at the newly created step sites more than compensates this energy penalty under FT conditions.

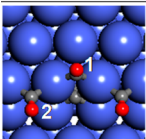
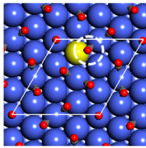
Figure 3 summarizes the calculated CO adsorption Gibbs free energies on terraces and near step sites. Two stable CO structures have been reported on Co(0001) terraces: a $\sqrt{3} \times \sqrt{3}$ and a $2\sqrt{3} \times 2\sqrt{3}$ structure (Figure 3a,b) with adsorption Gibbs free energies of –65 and –35 kJ/mol, respectively.^{39–41} To compare the stability of these structures, the adsorption free energies need to be multiplied by the respective coverages.⁴¹ This shows that the $\sqrt{3} \times \sqrt{3}$ structure ($-65 \times 1/3$ kJ/mol $\text{Co}_{\text{surface}}$) is marginally more stable than the $2\sqrt{3} \times 2\sqrt{3}$ -7CO structure ($-35 \times 7/12$ kJ/mol $\text{Co}_{\text{surface}}$) under Fischer–Tropsch conditions. Considering the 7/12 ML structure as the starting structure has a minor effect on the analysis and makes step creation more favorable. We will therefore consider (111) terraces covered with 1/3 ML CO as our starting structure.

For low step coverages, CO adsorbs stronger at the step edges than on the (111) terrace, and the top site is slightly preferred over the bridge site (Figure 3d,e). Experimentally, the formation of di- and tricarbonyl species where 2 or 3 CO molecules bind to the same Co atom have been suggested to stabilize step edges.^{1,42–44} We hence considered step coverages of 100% and higher at B5 and F4 sites. Several configurations were considered, and the structure where CO adsorbs at bridge sites (Figure 3k and 3m) was the most stable structure with an adsorption free energy of –78 kJ/mol at the B5 sites and –72 kJ/mol at the F4 sites. These values are essentially identical to the low-coverage values. In this structure, the CO molecules adopt a zigzag pattern to reduce through-space dipole–dipole repulsions. CO coverages higher than 100% are not thermodynamically favorable at the step sites, and the Gibbs free energy to adsorb for an additional CO at B5 steps with a

CO coverage of 100% (i.e., the structure in Figure 3l) is +43 kJ/mol, even though the *electronic* adsorption energy to adsorb the additional CO molecule is −22 kJ/mol.

Under Fischer–Tropsch conditions, it is favorable to occupy 50% of the B5 sites with square-planar carbon or with CH species. Surprisingly, the presence of square-planar carbon at the B5 sites increases the CO adsorption energy by 17 kJ/mol (Figure 3f), whereas CH at the B5 site has a limited effect on the CO adsorption energy (Figure 3g). The stronger CO adsorption is surprising because the same cobalt step atom now binds both carbon and CO. Such an attractive interaction is highly unusual considering the bond order conservation principle.⁴⁵ The unusual attraction is caused by the oxidation of the step cobalt atoms by square-planar carbon (see Table 1).

Table 1. CO Stretch Frequencies and Intensities, and Final State Co 2p Binding Energies for C/CO-Covered B5 Steps and for Co Terraces

Structure	CO frequency (cm ⁻¹) /intensity (km/mol)	Co 2p binding energy (eV)
	1843/1.7 – Bridge 1	779.6 – Co-step
	1781/0.1 – Bridge 2	777.8 – Co-terrace
	1986 / 0.3 – Top	778.3 – Co-top 777.8 – Co-bridge (indicated in yellow)
	1815 / 0.4	
	1814 / 0.5	
	1812/0.1	
	1811 / 0.8	
	1809 / 0.5	
	1805 / 0.1	

To achieve an aromatic electron count, the carbon atom withdraws electron density from the neighboring cobalt atoms.³² The reduced electron density on the cobalt atoms reduces the Pauli repulsion between the partially filled Co *d*_{z²} states and the filled CO 5σ orbital, as shown by Natural Bond Orbital analysis.⁴⁶ Also for a CO coverage of 100%, the presence of carbon strengthens CO adsorption by 10 kJ/mol (Figure 3m). The attractive interaction between carbon and CO *increases* the stability of the C/CO covered B5 step sites. Hydrogenation of the square-planar carbon atom becomes 16 kJ/mol unfavorable in the presence of CO. A similar attractive interaction is not found for the surface carbide. Note that the thermodynamic stability of O at the B5 sites (+41 kJ/mol) and at the terraces (−10 kJ/mol) is lower than the stability of C and CO, and is therefore not considered in our analysis.

Combining the stabilities in Figures 2 and 3 with the step creation energy, we can evaluate the overall thermodynamic driving force to create pairs of C and CO-covered B5 and F4 step sites or the formation of a surface carbide from CO-covered terraces under Fischer–Tropsch conditions. The argument follows a three-step Born–Haber cycle. First, 1/3 ML CO desorbs from the terrace sites to create a clean surface. Note that 3 terrace rows are converted to a row of B5 sites and a row of F4 sites (Figure 1b). Desorption costs 65 kJ/mol (i.e., 3 rows × 1/3 ML × 65 kJ/mol). The subsequent creation of a pair of step sites costs 85 kJ/mol. Finally, CO readsorbs at the new B5 and F4 step edges with 100% coverage and adsorption free energies of −78 and −72 kJ/mol, respectively. In our calculations, this overall process is thermoneutral. The increased CO adsorption energy and coverage at the step sites are hence *not* sufficient to drive the formation of steps or

nanoislands, and the presence of square-planar carbon at the B5 sites is an essential factor for step and island formation. Together, the stability of square-planar carbon and the increased CO adsorption energy enhance the driving force to form a pair of B5 and F4 steps to −19 kJ/mol. The creation of step edges from extended terraces hence becomes thermodynamically favorable under Fischer–Tropsch conditions, driving the breakup of cobalt terraces to form nanoislands, as observed by Wilson and De Groot.¹ The crucial role played by square-planar carbon is clearly illustrated by the absence of island formation in the experiments of Ehrensperger and Winterlin.⁹ For the conditions in their study (10 mbar and a H₂/CO ratio of 40), square-planar carbon is thermodynamically unstable (+12 kJ/mol) and hence does not form. Without the formation of square-planar carbon at the B5 step sites, step and island formation is unfavorable. A similar Born–Haber cycle can be constructed for the formation of a surface carbide. Our calculations show that the formation of a CO-covered carbide is marginally favorable for sufficiently large islands but significantly less favorable than the formation of C/CO covered steps and nanoislands under Fischer–Tropsch conditions. Indeed, the overall driving force to create a CO-covered cobalt carbide is only −0.5 kJ/mol Co_{surface}. In the *absence* of gas-phase CO, the formation of a surface carbide is more stable than the creation of carbon-covered steps, resulting in a carbon-induced restructuring of Co terraces, but not the formation of Co nanoislands, in agreement with experimental¹⁸ and recent DFT¹⁶ and molecular dynamics¹⁷ studies. Indeed, without the adsorption of CO, the stability gained by carbon adsorption at the B5 sites is not sufficient to overcome the step creation penalty (+85 kJ/mol). Thus, the creation of steps and nanoislands is not thermodynamically favorable in the absence of CO, explaining why Co nanoisland formation is not observed after ethylene decomposition.¹⁸ In summary, both CO and square-planar carbon are *required* to drive the formation of steps and nanoislands, and it is crucial to consider the adsorption of both CO and carbon in a thermodynamic analysis.

To allow experimental detection of the predicted C/CO-covered step sites, CO stretch frequencies and IR intensities, as well as Co 2p and C 1s binding energies were computed and compared with values for terrace sites (Table 1). For CO at the carbon-covered B5 sites, two frequencies are computed: 1843 cm⁻¹ for CO at the carbon-free site and 1781 cm⁻¹ for CO at the site with carbon. The large difference in the calculated intensity suggests that only the 1843 cm⁻¹ frequency could be observed. Since this frequency differs significantly from the range computed for bridge CO in the 2√3 × 2√3 structure, 1805–1815 cm⁻¹, and from the low-coverage value of 1751 cm⁻¹, it might be an experimental fingerprint of CO at carbon-covered B5 sites. The C 1s binding energy for the C/CO-covered B5 sites, 283.0 eV, is typical for Co carbide species,^{11,30} and close to the value calculated for a p4g Co carbide, 282.7 eV. The Co 2p binding energy for the C/CO-covered B5 sites, 779.6 eV, falls in the range of cobalt oxides (~780 eV⁴⁷) and differs significantly from the value for a clean (777.8 eV) and for a CO-covered (778.3 eV) surface. To confirm that the Co 2p binding energy for C/CO-covered steps resembles the value for CoO, we used LDA + U (U = 4.2 eV⁴⁸) to compute both binding energies. With this approach, very similar Co 2p binding energies of 779.6 and 779.9 eV were indeed computed for CoO and for C/CO-covered B5 sites, respectively. We hence speculate that the recent observation of the development

of a minor Co oxidation component during the induction period when the Co catalyst gains Fischer–Tropsch activity^{11,49} is related to the formation of the C/CO-covered step sites and nanoislands predicted in this study.

CONCLUSIONS

Cobalt catalysts undergo a massive surface reconstruction under Fischer–Tropsch conditions to form nanoislands. The driving force for the formation of step sites and nanoislands, as well as the structure and coverage of the step sites were studied using density functional theory. Although the energy penalty to create a pair of B5 and F4 step sites and to desorb CO from the terrace sites that create the steps is substantial, the unusual stability of square-planar carbon at the B5 steps and the increased CO adsorption energy and high CO coverage at the step sites together make it highly favorable to create step sites and islands under Fischer–Tropsch conditions. When either CO adsorption or square-planar carbon adsorption are ignored, step and island creation is not thermodynamically favorable. Aromatic square-planar carbon hence plays a crucial role in the structure, coverage, and activity of Co Fischer–Tropsch catalysts. Its stability and bonding pattern furthermore suggests that this unique role is not limited to cobalt and should also be explored (e.g., for Ni, Fe, Rh, and Pd).^{33–37} The Co 2p binding energy at the C/CO-covered step sites, 779.6 eV, is typical for oxidized Co species and could be a fingerprint for the predicted structures. The eventual shape and size of the nanoislands also depends on the stability and coverage of corner sites, and these are likely a strong function of the reaction conditions. Insight into the structure, the coverage, and the formation of these nanoislands will constitute the basis to analyze the reaction mechanism at these sites.

AUTHOR INFORMATION

Corresponding Author

*E-mail: Mark.Saeyns@UGent.be.

Notes

The authors declare no competing financial interest.

ACKNOWLEDGMENTS

This work was supported by Shell Global Solutions and by a Faculty Strategic Funding Initiative from the National University of Singapore

REFERENCES

- (1) Wilson, J.; de Groot, C. J. *Phys. Chem.* **1995**, *99*, 7860–7866.
- (2) Hansen, P. L.; Wagner, J. B.; Helveg, S.; Rostrup-Nielsen, J. R.; Clausen, B. S.; Topsøe, H. *Science* **2002**, *295*, 2053–2055.
- (3) Yoshida, H.; Kuwauchi, Y.; Jinschek, J. R.; Sun, K.; Tanaka, S.; Kohyama, M.; Shimada, S.; Haruta, M.; Takeda, S. *Science* **2012**, *335*, 317–319.
- (4) Tao, F.; Dag, S.; Wang, L. W.; Liu, Z.; Butcher, D. R.; Bluhm, H.; Salmeron, M.; Somorjai, G. A. *Science* **2010**, *327*, 850–852.
- (5) Venvik, H. J.; Berg, C.; Borg, A. *Surf. Sci.* **1998**, *402*, 57–61.
- (6) Venvik, H. J.; Borg, A.; Berg, C. *Surf. Sci.* **1998**, *397*, 322–332.
- (7) van Hardeveld, R.; Hartog, F. *Surf. Sci.* **1969**, *15*, 189–230.
- (8) Shetty, S.; van Santen, R. A. *Catal. Today* **2011**, *171*, 168–173.
- (9) Ehrensperger, M.; Wintterlin, J. *J. Catal.* **2014**, *319*, 274–282.
- (10) Prieto, G.; Martínez, A.; Concepción, P.; Moreno-Tost, R. J. *Catal.* **2009**, *266*, 129–144.
- (11) Tan, K. F.; Xu, J.; Chang, J.; Borgna, A.; Saeys, M. J. *Catal.* **2010**, *274*, 121–129.
- (12) Gong, X. Q.; Raval, R.; Hu, P. *Surf. Sci.* **2004**, *562*, 247–256.
- (13) Gong, X. Q.; Raval, R.; Hu, P. *J. Chem. Phys.* **2005**, *122*, 024711.
- (14) Weststrate, C. J.; Ciobica, I. M.; Saib, A. M.; Moodley, D. J.; Niemantsverdriet, J. W. *Catal. Today* **2014**, *228*, 106–112.
- (15) Ciobica, I. M.; van Santen, R. A.; van Berge, P. J.; van de Loosdrecht, J. *Surf. Sci.* **2008**, *602*, 17–27.
- (16) Corral Valero, M.; Raybaud, P. *J. Phys. Chem. C* **2014**, *118*, 22479–22490.
- (17) Zhang, X.; van Santen, R. A.; Hensen, E. J. M. *ACS Catal.* **2015**, *5*, 596–601.
- (18) Weststrate, C. J.; Kazalkaya, A. C.; Rossen, E. T. R.; Verhoeven, M. W. G. M.; Ciobica, I. M.; Saib, A. M.; Niemantsverdriet, J. W. *J. Phys. Chem. C* **2012**, *116*, 11575–11583.
- (19) den Breejen, J. P.; Radstake, P. B.; Bezemer, G. L.; Bitter, J. H.; Frøseth, V.; Holmen, A.; de Jong, K. P. *J. Am. Chem. Soc.* **2009**, *131*, 7197–7203.
- (20) Zhuo, M.; Borgna, A.; Saeys, M. *J. Catal.* **2013**, *297*, 217–226.
- (21) Zhang, Y.; Yang, W. *Phys. Rev. Lett.* **1998**, *80*, 890.
- (22) Dion, M.; Rydberg, H.; Schröder, E.; Langreth, D. C.; Lundqvist, B. I. *Phys. Rev. Lett.* **2004**, *92*, 246401.
- (23) Klimeš, J.; Bowler, D. R.; Michaelides, A. *Phys. Rev. B: Condens. Matter Mater. Phys.* **2011**, *83*, 195131.
- (24) Blöchl, P. E. *Phys. Rev. B: Condens. Matter Mater. Phys.* **1994**, *50*, 17953–17979.
- (25) Kresse, G.; Furthmüller, J. *Comput. Mater. Sci.* **1996**, *6*, 15–50.
- (26) Kresse, G.; Furthmüller, J. *Phys. Rev. B: Condens. Matter Mater. Phys.* **1996**, *54*, 11169–11186.
- (27) Smith, J. M.; van Ness, H. C.; Abbott, M. M. *Introduction to Chemical Engineering Thermodynamics*, 6th ed.; Mc Graw Hill: New York, 2001; p 383.
- (28) Giannozzi, P.; Baroni, S. *J. Chem. Phys.* **1994**, *100*, 8537–8539.
- (29) Kohler, L.; Kresse, G. *Phys. Rev. B: Condens. Matter Mater. Phys.* **2004**, *70*, 165405.
- (30) Trinh, Q. T.; Tan, K. F.; Borgna, A.; Saeys, M. *J. Phys. Chem. C* **2013**, *117*, 1684–1691.
- (31) Kittel, C. *Introduction to Solid State Physics*, 8th ed.; John Wiley and Sons Inc: New York, 2005; p 50.
- (32) Nandula, A.; Trinh, Q. T.; Saeys, M.; Alexandrova, A. N. *Angew. Chem., Int. Ed.* **2015**, *54*, 5312–5316.
- (33) Hoffmann, R.; Alder, R. W.; Wilcox, C. F., Jr. *J. Am. Chem. Soc.* **1970**, *92*, 4992–4993.
- (34) Schleyer, P. v. R.; Boldyrev, A. I. *J. Chem. Soc., Chem. Commun.* **1991**, *21*, 1536–1538.
- (35) Li, X.; Zhang, H. F.; Wang, L. S.; Geske, G. D.; Boldyrev, A. I. *Angew. Chem., Int. Ed.* **2000**, *39*, 3630–3632.
- (36) Boldyrev, A. I.; Li, X.; Wang, L. S. *Angew. Chem., Int. Ed.* **2000**, *39*, 3307–3309.
- (37) Alexandrova, A. N.; Nayhouse, M. J.; Huynh, M. T.; Kuo, J. L.; Melkonian, A. V.; Chavez, G.; Hernando, N. M.; Kowal, M. D.; Liu, C. P. *Phys. Chem. Chem. Phys.* **2012**, *14*, 14815–14821.
- (38) Kirsch, J. E.; Harris, S. *Surf. Sci.* **2003**, *522*, 125–142.
- (39) Papp, H. *Surf. Sci.* **1983**, *129*, 205–218.
- (40) Bridge, M. E.; Comrie, C. M.; Lambert, R. M. *Surf. Sci.* **1977**, *67*, 393–404.
- (41) Gunasooriya, G. T. K. K.; van Bavel, A. P.; Kuipers, H. P. C. E.; Saeys, M. *Surf. Sci.*, DOI: [10.1016/j.susc.2015.06.024](https://doi.org/10.1016/j.susc.2015.06.024).
- (42) Rygh, L. E. S.; Ellestad, O. H.; Klæboe, P.; Nielsen, C. J. *Phys. Chem. Chem. Phys.* **2000**, *2*, 1835–1846.
- (43) Beitel, G. A.; Laskov, A.; Oosterbeek, H.; Kuipers, E. W. *J. Phys. Chem.* **1996**, *100*, 12494–12502.
- (44) Beitel, G. A.; de Groot, C. P. M.; Oosterbeek, H.; Wilson, J. H. *J. Phys. Chem. B* **1997**, *101*, 4035–4043.
- (45) Shustorovich, E. *Surf. Sci. Rep.* **1986**, *6*, 1–63.
- (46) Banerjee, A.; Zhuo, M.; Saeys, M.; *in preparation, to be submitted*.
- (47) Biesinger, M. C.; Payne, B. P.; Grosvenor, A. P.; Lau, L. W. M.; Gerson, A. R.; Smart, R. S. *Appl. Surf. Sci.* **2011**, *257*, 2717–2730.
- (48) Youmbi, B. S.; Calvayrac, F. *Surf. Sci.* **2014**, *621*, 1–6.
- (49) Tsakoumis, N. E.; Voronov, A.; Ronning, M.; van Beek, W.; Borg, O.; Rytter, E.; Holmen, A. *J. Catal.* **2012**, *291*, 138–148.